

## INFLUENCE OF PHOTOEXCITATION ON THE PARAMETERS OF SURFACE POTENTIAL BARRIER

In this work the effect of photoexcitation on the parameters of surface potential barrier is investigated. We have examined in detail the phenomenon, which is determined by trapping of nonequilibrium carriers into the deep levels. It is shown how the parameters of surface barrier are governed by visible excitation. The described effect together with the usage of an asymmetric heterojunction permits the fabrication of an image sensor of a quite new type.

### 1. Introduction

The development of innovations in the operating physical principles, design and technology of electronic devices based on non-crystalline materials to be a significant part of investigations completing the traditional work with monocrystalline ideal semiconductors. The main strategy of semiconductor electronics is to design and fabricate devices made from pure and perfect materials. Such an approach gives rise to the appearance of various arrangement that are successfully used in common. One of the most impressive results is an optical image sensor based on the CCD imaging chip. Orientation toward the most perfect crystals does not allow all the requirements of modern techniques to be satisfied. Very often either a device with a large working surface or a large array of devices is needed. For such a purpose polycrystalline or amorphous materials, fabricated by different technologies, are employed. As a rule, devices based on these materials do not have the same physical principle of operation as the crystalline ones. For instance, electron tubes with a variety of semiconductor layers of high luminescence and photocathode characteristics are used to develop large-area image sensors for X-ray applications. Of course, it is impossible to create a polycrystalline CCD image sensor with a similar large sensitive surface, although no limitations, relative to the matrix array size, exist for the operation principle of a CCD.

### 2. Theory

A contact between two semiconducting materials, one or both of which are thin-film semiconductors is one of the interesting structures of non-crystalline electronics. We have investigated in detail CdS—Cu<sub>2</sub>S heterojunction. In particular, this heterojunction was employed as the basis for a thin-film solar cell, but as is evident from our investigation such a device has wider applications that follow directly from disorder effects of such a structure. Fig. 1 shows an energy-band diagram of the CdS—Cu<sub>2</sub>S

heterojunction. This heterojunction is a contact between two semiconductors with a lattice mismatch

of about 4%. This mismatch leads to a strong disorder of the regular lattice structure in the regions near the interface. This distinctive feature is that the CdS region, where the space charge is localized, possesses a material with long-range disorder, and consequently with non-zero density  $N(E)$  of the localized gap states. Such a property is absolutely distinct from the properties of ideal GaAs—AlGaAs structures and has a strong effect on the photoelectrical characteristics of the heterojunction.

During exposure of the sample to light quanta of sufficient energy, non-equilibrium minority carriers are captured by the localized states in CdS. We can see that even low-level excitation (for which the density of non-equilibrium carriers  $\Delta n$  is much smaller than that of equilibrium carriers  $n_0$ ) changes the parameters of the heterojunction drastically [1].

Let us consider the special distribution of the trapped holes as

$$\Delta p(x) = \Delta p_0 e^{\frac{\varphi_0}{kT} \left(1 - \frac{x}{W}\right)}, \quad (1)$$

where  $\Delta p_0$  is concentration of non-equilibrium holes, captured by the local centres within the quasineutral region of CdS, and  $W$  and  $\varphi_0$  are CdS barrier width and height, respectively. Then the space-charge distribution function  $\rho(x)$  is

$$\rho(x) = e \left[ N_d + \Delta p_0 e^{\frac{\varphi_0}{kT} \left(1 - \frac{x}{W}\right)} \right], \quad (2)$$

where  $N_d$  represents ionized donor concentration in CdS.

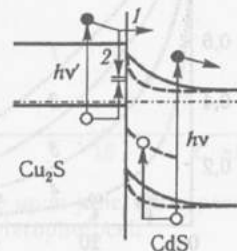


Fig. 1. Band diagram of CdS—Cu<sub>2</sub>S heterojunction:

1 — transition of electrons, excited with  $h\nu$  photons in Cu<sub>2</sub>S, across the junction plane; 2 — surface recombination. Dashed line represent the band profiles under CdS band-gap illumination  $h\nu$

From the analytic solution of Poisson's equation for such a dependence, it can be shown that for  $x \ll W$ , i. e. near the interface

$$\phi(x) = A(N_d, \Delta\rho_0, \xi) \left[ e^{\xi(1-\frac{x}{W})} - 1 \right], \quad (3)$$

where  $A$  is some constant dependent on the density of uncompensated donors in  $n$ -type material and values  $\Delta\rho_0$  and  $\xi = \phi_0/kT$  as parameters.

The main result here is that even a low illumination level changes the electron energy spatial distribution from a parabolic to an exponential one, thus increasing the electric field near the interface. Fig. 2 illustrates the computational dependencies of the potential variation  $\phi(x)$  near heterojunction interface under various irradiation conditions.

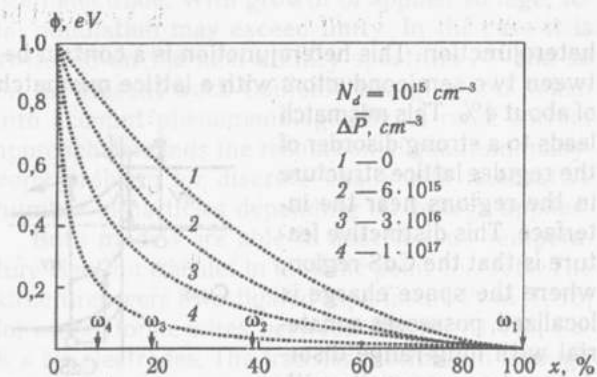


Fig. 2. Spatial distribution of the potential variation  $\phi(x)$  in space charge region of heterojunction, calculated for different densities of trapped photogenerated holes. The arrows indicate barrier widths, corresponding to curves 1—4

It should be mentioned that non-equilibrium state of the heterojunction possesses a long time stability [1]. When excitation is turned off, slow emission of non-equilibrium holes from region of space-charge layer begins. The rate of the emission process is governed by the type of the trapping centers. When minority-carrier trapping centers dominates, the time constant  $\tau_t$  of the process is determined by thermal escape probability  $\gamma_t$  of the centers

$$\frac{1}{\tau_t} = \gamma_t = P_v v_p \sigma_p e^{-\frac{E_t}{kT}}, \quad (4)$$

where  $P_v$  is density of hole states in valence band of CdS,  $\sigma_p$  is trap depth and  $v_p$  is thermal velocity for holes.

If the non-equilibrium holes in the space-charge layer are captured by the recombination centers, the time constant for heterojunction transient from the excited to the equilibrium state will be defined by electron-hole recombination velocity  $S_r$ . The occurrence of potential barrier in cadmium sulfide leads to spatial separation of electrons and holes, generated in CdS under illumination of heterojunction. During illumination the photoexcited holes moves toward the interface, where they are promptly trapped by deep levels, whereas electrons are swept

out of barrier region into CdS bulk. So the situation is closed to that of the phenomenon of «stored photoconductivity». In order to re-establish the equilibrium, the photoexcited carriers have to go over potential recombination barrier which height is  $\phi_0$ . In this case, life time of photoexcited holes with recombination centers becomes extremely large and is given by

$$\tau_p = \tau_p^0 e^{\frac{\phi_0}{kT}}, \quad (5)$$

where  $\tau_p^0 = \frac{1}{v_n \sigma_n n}$ , is lifetime of holes with recombination centers in bulk of CdS.

It must be emphasized that trapped non-equilibrium charge is stable not only over time, but possesses a spatial stability, also. To clear this point we must remember that lifetime of free non-equilibrium holes  $\tau_p$  is about  $10^{-9}$  s. From Einstein relation

$$\frac{D_p}{kT} = \frac{\mu}{e} \quad (6)$$

noting that hole mobility in CdS is of  $1 \text{ cm}^2/V \cdot \text{s}$ , we can obtain the diffusion length for holes  $L_p$

$$L_p = (D_p \tau_p)^{1/2} = 0,05 \text{ } \mu\text{m}. \quad (7)$$

Therefore, the holes are being captured by local centers in space-charge region within a distance less than  $0,05 \text{ } \mu\text{m}$  from the place they were generated. As we have mentioned earlier, thermal emission from traps is weak and followed by immediate re-trapping.

When heterojunction is nonuniformly illuminated, an inhomogeneous distribution of space-charge is established over working surface of heterojunction. This space-charge distribution is essentially given by local illumination of surface areas.

Our interest to space-charge distribution  $\rho(x)$  and potential distribution  $\phi(x)$  arises because of charge collection efficiency from  $p$ -type material (in our case  $\text{Cu}_2\text{S}$ ) related to the dependencies

$$I_{sc} = I_{sc}^0 \frac{\frac{\mu_n}{e} \frac{d\phi(x)}{dx} \Big|_{x=0}}{\frac{\mu_n}{e} \frac{d\phi(x)}{dx} \Big|_{x=0} + S_r}. \quad (8)$$

Here  $I_{sc}$  is short-circuit photocurrent in heterojunction, the  $I_{sc}^0$  is current in the absence of interface recombination losses,  $S_r$  is surface recombination velocity.

The electrons, photoexcited in  $\text{Cu}_2\text{S}$ , can either recombine with interface states or be separated from holes under the action of barrier field, localized in CdS. The relationship between interface recombination velocity  $S_r$  and electron drift velocity  $v_d = \frac{\mu_n}{e} \frac{d\phi(x)}{dx} \Big|_{x=0}$  for the noticed processes determines the magnitude of current  $I_{sc}$  and real cell efficiency. The variation in the spatial dependence  $\phi(x)$  with CdS band gap illumination strongly influences the drift velocity of electrons in barrier region, consequently increasing charge collection efficiency.

Here, one must bear in mind that we are dealing with collection efficiency of non-equilibrium electrons, excited in  $p$ -type semiconductor  $\text{Cu}_2\text{S}$  and moving across the junction plane. Thus, as is evident from eq. (8), the current generated in  $p$ -type material is dependent on illumination conditions in type material.

This means that photocurrent, produced by excitation of heterojunction simultaneously with two light beams, one of which is from IR range and absorbs in  $\text{Cu}_2\text{S}$ , and the other from the visible range and absorbs in  $\text{CdS}$ , does not equal to the sum of photocurrents resulting from the illumination of heterojunction with each of the beams separately. The above-mentioned effects is of great importance for us. We have called this phenomenon the non-additive formation of current effect, i. e., the NAFC effect.

For solar cells based on  $\text{CdS}-\text{Cu}_2\text{S}$ , the NAFC effect has the negative character, so it was of no interest to researchers. Our investigations, however, reveal that the effect, which is a problem for a solar cell, may be turned to advantage and successfully used for manufacturing an innovative image sensor [2–5].

### 3. Experimental results

Let us examine the experimental data that allow the proposed model to be confirmed. The most direct way to determine the characteristics of space-charge layer of the heterojunction is to measure the corresponding changes in junction capacitance  $C_b$  as a function of various factors. Junction capacitance as a function of the exciting light wavelength is illustrated in fig. 3. As is evident from curve 1 in fig. 3, if heterojunction base layer ( $\text{CdS}$ ) of thickness  $10 \mu\text{m}$

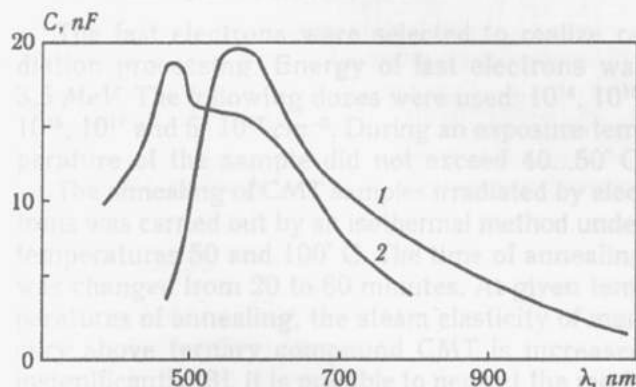


Fig. 3. Spectral dependencies of the barrier capacitance in thin film  $\text{CdS}-\text{Cu}_2\text{S}$  heterojunction:

1 — illumination from the side  $10 \mu\text{m}$  thick  $\text{CdS}$  layer; 2 — illumination from the side  $0,2 \mu\text{m}$  thick  $\text{Cu}_2\text{S}$  layer

is directed toward the illumination, the well-known photoresponse for  $\text{Cu}$ -doped  $\text{CdS}$ , resulting from impurity carrier generation, in our case also peaks at about  $600 \text{ nm}$ . In this case intrinsic light does not reach the interface yet. From curve 2 in fig. 3, corresponding to the illumination of heterojunction from the side of  $0,2 \mu\text{m}$  thick  $\text{Cu}_2\text{S}$  layer, intrinsic-carrier-generation peak at  $500 \text{ nm}$  can be seen as

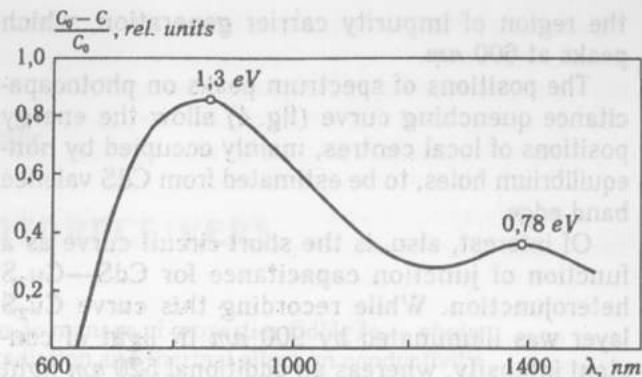


Fig. 4. Photocapacitance quenching spectrum:  $C_0$  is junction capacitance resulting from illumination of heterojunction with  $\lambda = 560 \text{ nm}$

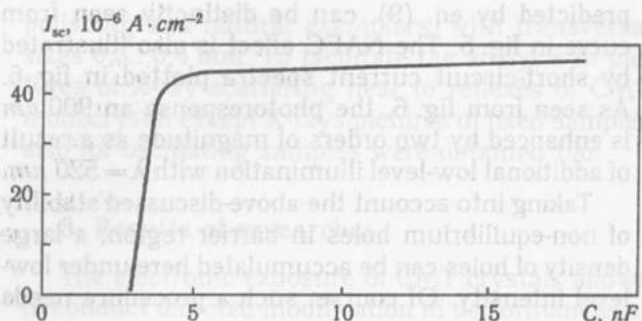


Fig. 5. Short current dependence upon junction capacitance in  $\text{CdS}-\text{Cu}_2\text{S}$  heterophotocell

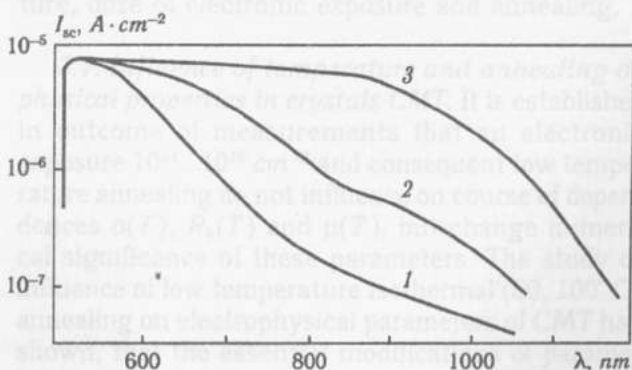


Fig. 6. Increase of photosensitivity in  $\text{CdS}-\text{Cu}_2\text{S}$  heterojunction during low-level additional excitation with  $\lambda = 520 \text{ nm}$ . Curve 1 is without additional excitation. Illumination level of additional excitation increases with the curve number

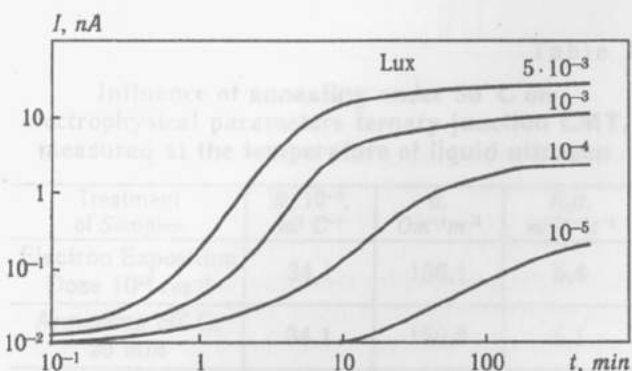


Fig. 7. Increase of sensor photocurrent with time during the adsorption of photons ( $1,9 \text{ eV}$ ) for various levels of illumination at  $300 \text{ K}$

the region of impurity carrier generation, which peaks at 600 nm.

The positions of spectrum peaks on photocapacitance quenching curve (fig. 4) allow the energy positions of local centres, mainly occupied by non-equilibrium holes, to be estimated from CdS valence band edge.

Of interest, also, is the short-circuit curve as a function of junction capacitance for CdS—Cu<sub>2</sub>S heterojunction. While recording this curve Cu<sub>2</sub>S layer was illuminated by 900 nm IR light of constant intensity, whereas an additional 520 nm light provides an increase of barrier capacitance. Here the photocurrent obtained in the presence of exciting light only with  $\lambda = 520$  nm was subtracted from the measured current value. The saturation of current, predicted by eq. (9), can be distinctly seen from curve in fig. 5. The NAFC effect is also illustrated by short-circuit current spectra plotted in fig. 6. As seen from fig. 6, the photoresponse at 900 nm is enhanced by two orders of magnitude as a result of additional low-level illumination with  $\lambda = 520$  nm.

Taking into account the above-discussed stability of non-equilibrium holes in barrier region, a large density of holes can be accumulated here under low-level intensity. Of course, such a procedure needs

a lot of time. Note that photosensitivity of CdS—Cu<sub>2</sub>S heterojunction resembles that of a photoemulsion where a latent image is being formed. As shown in fig. 7 for CdS—Cu<sub>2</sub>S heterojunction, photoreponse at  $\lambda = 900$  nm is modulated by short-wavelength illumination. Thus, we can state that the results obtained satisfy well the above-discussed model of non-ideal heterojunction.

#### References

1. Vassilevski D. L., Borschak V. A., Vinogradov M. S. Influence of tunnel effects on the kinetics of the photocapacitance in nonideal heterojunctions // *Solid-State Electronics*. — 1994. — Vol. 37, № 9. — P. 1680—1682.
2. Vassilevski D. L., Borschak V. A., The utilisation of a sensor based on a heterojunction for astronomy // *Proc. ICO-16 Satellite Conf. on Active and Adaptive Optics*, Garching—Munich, Germany, 2—5 Aug. — 1993. — P. 377.
3. Vassilevski D. L., Borschak V. A., Victor P. A., Vinogradov M. S., Zatoovskaya N. P. A novel heterojunction-based low-illumination image sensor, with applications to astronomy // *Sensors and Actuators A*. — 1994. — 45. — 191.
4. Borschak V., Golovanov V., Stankova E., Zatoovskaya N. Novel Image Sensor for visible and X-ray Spectra» *Euroensors XI*, conf. Warsaw, Poland, September 21—24, 1997.
5. Vassilevski D. L., Vinogradov M. S., Borschak V. A. Photon induced modulation of surface barrier: investigation and application for a new image sensor // *Applied Surface Science*. — Dec. 1996. — 103(4). — P. 383—389.

Fig. 5. Short current dependence upon junction capacitance in CdS—Cu<sub>2</sub>S heterojunction.

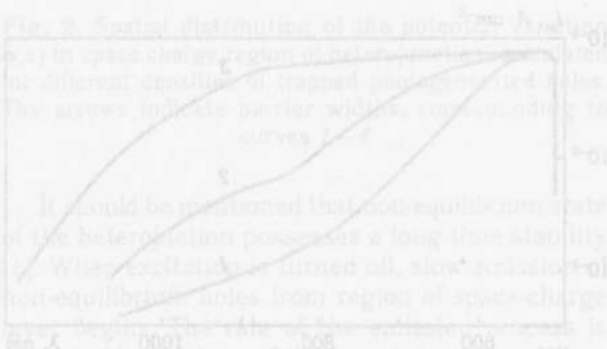


Fig. 6. Factors of photosensitivity in CdS—Cu<sub>2</sub>S heterojunction during low-level additional excitation with  $\lambda = 520$  nm. Curve 1 is without additional excitation. The number of additional excitation increases with the curve number.

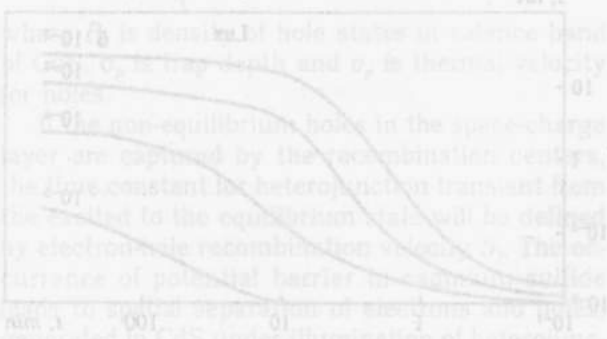


Fig. 7. Increase of sensor photocurrent with time during the absorption of photons (1.9 eV) at various levels of illumination at 500 K peak by defect

Fig. 8. Spectral dependence of the barrier capacitance in thin film CdS—Cu<sub>2</sub>S heterojunction. The x-axis is labeled 'lambda' and the y-axis is labeled 'C\_b'. The curve shows a peak around 600 nm.

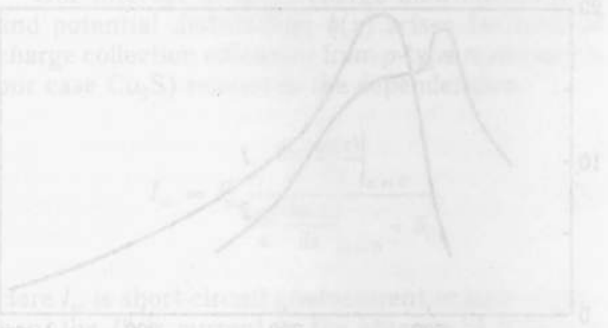


Fig. 9. Short-circuit current spectra plotted in fig. 6. As seen from fig. 6, the photoresponse at 900 nm is enhanced by two orders of magnitude as a result of additional low-level illumination with lambda = 520 nm.